



EARTH SCIENCES

Geochemistry and $\delta^{11}\text{B}$ evolution of tourmaline from tourmalinite as a record of oceanic crust in the Tonian Ibaré ophiolite, southern Brasiliano Orogen

KARINE R. ARENA, LÉO A. HARTMANN, CRISTIANO LANA, GLÁUCIA N. QUEIROGA & MARCO P. CASTRO

Abstract: The isotopic and geochemical evolution of tourmaline constrain the processes of paleo-oceanic lithosphere in ophiolites. The Brasiliano Orogen is a major structure of South America and requires characterization for the understanding of Gondwana supercontinent evolution. We made a pioneering investigation of tourmaline from a tourmalinite in the Ibaré ophiolite by integrating field work with chemical analyses of tourmaline by electron microprobe (EPMA) and $\delta^{11}\text{B}$ determinations via laser ablation inductively coupled plasma mass spectrometer (LA-ICP-MS). Remarkably massive tourmalinite (>90 vol.% tourmaline, some chlorite) enclosed in serpentinite has homogeneous dravite in chemical and isotopic composition ($\delta^{11}\text{B} = +3.5$ to $+5.2\text{‰}$). These results indicate a geotectonic environment in the altered oceanic crust for the origin of the tourmalinite. This first $\delta^{11}\text{B}$ characterization of tourmaline from tourmalinite sets limits to the evolution of the Neoproterozoic to Cambrian Brasiliano Orogen and Gondwana evolution.

Key words: boron isotopes, geochemistry, Ibaré ophiolite, tourmalinite, southern Brasiliano Orogen.

INTRODUCTION

Tourmaline is a most useful mineral because it is robust and can retain a record of geological processes (van Hinsberg et al. 2011). The mineral is helpful for understanding both continental (Chaussidon & Albarède 1992, Trumbull et al. 2008, Cabral et al. 2017) and oceanic (Smith et al. 1995, Farber et al. 2015) settings.

Most studies focused on accessory tourmaline in granitic and mineralized volcanic-sedimentary rocks, including sulphide ore (e.g., Namaqualand, South Africa - Plimer 1987, Sullivan, British Columbia - Palmer & Slack 1989, Broken Hill, Australia - Slack et al. 1993). Fewer studies concentrated on oceanic lithosphere,

including crust and mantle or on volatile transfer processes from the subduction setting to the mantle wedge and arc magmatism (Palmer 1991, Rosner et al. 2003, Savov et al. 2005, Boschi et al. 2008, Yamaoka et al. 2012). In Brazil, stratiform tourmalinite occurs associated to mineralized quartz-tourmaline veins in the Calymmanian Serra do Itaberaba (Ribeira belt, SE Brazil - Garda et al. 2009). Tourmaline was also described in pegmatites (Borborema Province, NE Brazil - Trumbull et al. 2013) and as platiniferous gold-tourmaline aggregates (Gold-palladium belt of Minas Gerais, Brazil - Cabral et al. 2017).

Tourmaline (geochemistry, $\delta^{11}\text{B}$) was only studied in continental rocks in the continent, not in ophiolites. In the Brasiliano Orogen

Neoproterozoic ophiolites were studied with zircon U-Pb isotopes in the Araçuaí Belt (oceanic plagiogranite – Queiroga et al. 2007) and Dom Feliciano Belt (albitite, chloritite, tourmalinite, rodingite blackwall – Arena et al. 2016, 2017, 2018). Tourmalines from ophiolites were not studied.

We selected a massive tourmalinite (>90 vol.% tourmaline) from southern Brazil, because the rock is part of the Ibaré ophiolite. The sample was previously investigated with zircon U-Pb-Hf isotopes by Arena et al. (2017). Large (5-30 m diameter) tourmalinites remain undescribed in the oceanic crust or ophiolites, so this is a pioneering investigation of mantle interaction with oceanic water in the Tonian.

The tourmalinite was described in the field and large tourmaline crystals (up to 10 cm) were studied by EPMA for major elements and LA-ICP-MS for $\delta^{11}\text{B}$. The results indicate a remarkably homogeneous dravite, including boron isotopes ($\delta^{11}\text{B} = +3.5$ to $+5.2\%$). We interpret the tourmalinite as formed in the Tonian oceanic crust by alteration of mantle rocks in contact with oceanic water. This characterization of the geotectonic environment may have large impact on studies of the Early Brasiliano Orogen in the continent and reconstruction of Rodinia and Gondwana.

MATERIALS AND METHODS

Field study of the Ibaré ophiolite included collection of selected tourmalinite IB14 sample. Petrography of the tourmalinite preceded the determination of chemical and boron isotopic analyses of tourmaline. Petrography was done with a transmission petrographic microscope Olympus BX51, UC30. One polished thin section of the sample was studied for elemental mapping of tourmaline by electron microprobe at Laboratório de Microsonda Eletrônica,

Universidade Federal do Rio Grande do Sul. A block was cut from the massive tourmalinite sample (Figs. 2d, e) and measures 10 cm in length by ~1.5 cm in width. The block was divided into parts and placed in 5 mounts in sequential order, each measuring 2 cm x 1.5 cm (Fig. 2f). Mounts from tablets 3 and 4 (Figs. 2f, 3a, b) were selected for analyses by scanning electron microprobe and boron isotopes at Departamento de Geologia, Universidade Federal de Ouro Preto (UFOP), Minas Gerais. All these spot analyses were controlled by backscattered electron images (Fig. 3).

Electron microprobe

Electron microprobe analyses of mounted tourmalines were performed at UFOP using a JEOL JXA-8230 Superprobe equipped with 5 spectrometers. Operating conditions were 15 kV accelerating voltage, 20 nA beam current and 10 μm beam diameter and a selection of measurement spots ensured that the stimulated volume was not contaminated by phases other than tourmaline. Counting times on the peaks/background were 10/5 s for all elements. Background intensities were collected at higher and lower energies relative to the corresponding $K\alpha$ line. Appropriate natural and synthetic reference materials were used for calibration (Supplementary Material - Table S1). Tourmaline structural formulae were calculated by normalizing to 15 cations in the tetrahedral and octahedral sites ($T + Z + Y$) and assuming 3 boron apfu (Henry et al. 2011) using the Excel spreadsheet of Tindle et al. (2002).

Boron isotopes

Boron isotope ratio measurements were carried out at UFOP on a Thermo-Scientific Neptune Plus multi-collector ICP-MS coupled to a Photon Machines 193 Excimer laser ablation system. Samples were ablated in He atmosphere using

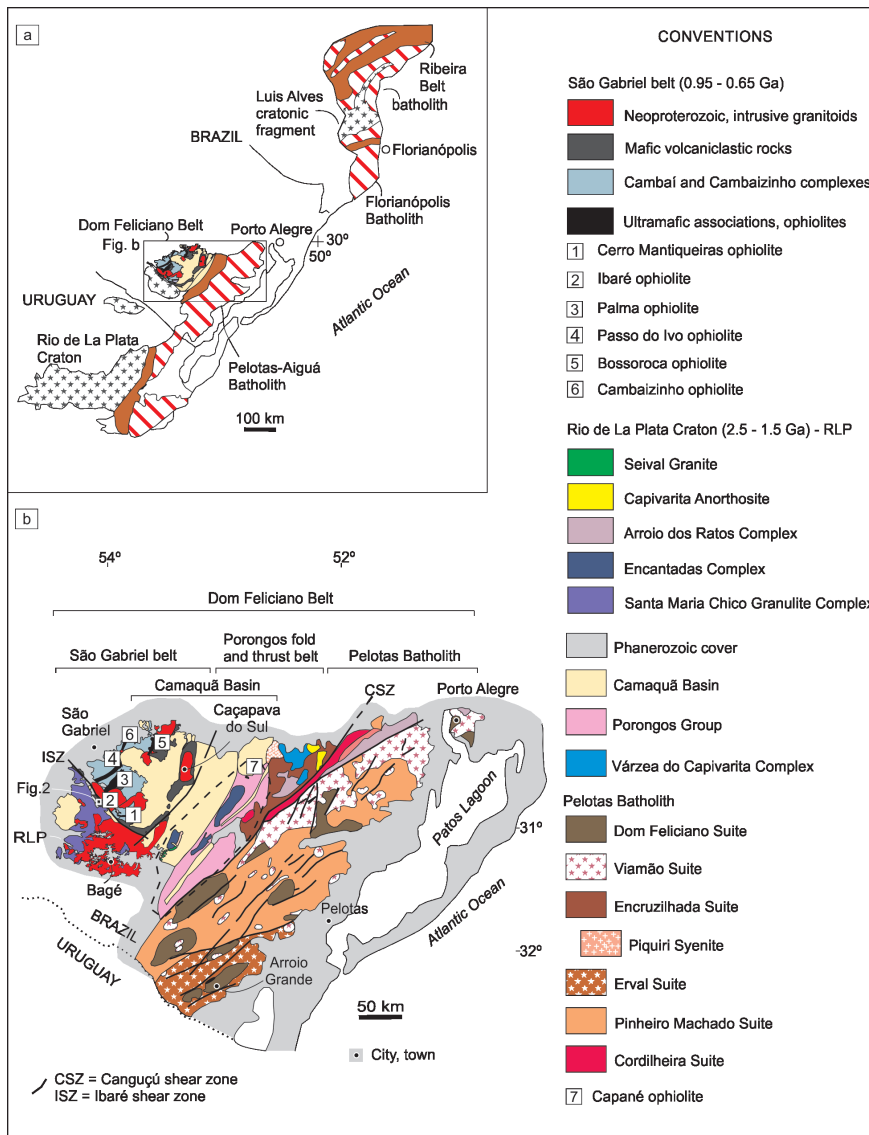


Figure 1. (a) Main tectonic units of southern Brazil and Uruguay (adapted from Rapela et al. 2007, Chemale et al. 2011); (b) Geological map of Dom Feliciano Belt and basement (after Philipp et al. 2013, Pertille et al. 2015, Arena et al. 2017). Location of Figure 2 indicated.

20 μm diameter spot and 15 Hz frequency at 7 J/cm². In the mass spectrometer, ¹⁰B and ¹¹B intensities were measured (in low resolution) on the L2 and H2 detectors, respectively. The measurements consisted of 98 cycles (or integration) and 0.5 s of integration time. Data were processed after the daily run using an in-house spreadsheet by A. Gerdes (e.g., Devulder et al. 2015). The measured, background signal of the unknown sample was corrected for instrumental mass fractionation (IMF) using

a standard-sample bracketing method and tourmaline B4 (schorlite, $\delta^{11}\text{B} = -8.62 \text{ ‰}$) (Tonarini et al. 2003) as the primary reference material. The drift-corrected ratios were referenced to the published ¹¹B/¹⁰B value of the reference material and the results are reported as $\delta^{11}\text{B}$ values relative to NIST SRM 951 boric acid using the certified ¹¹B/¹⁰B value of 4.04362 ± 0.00137 (Catanzaro et al. 1970). Matrix effects, known to occur in B isotope measurements (e.g., Mikova et al. 2014) and the reproducibility of

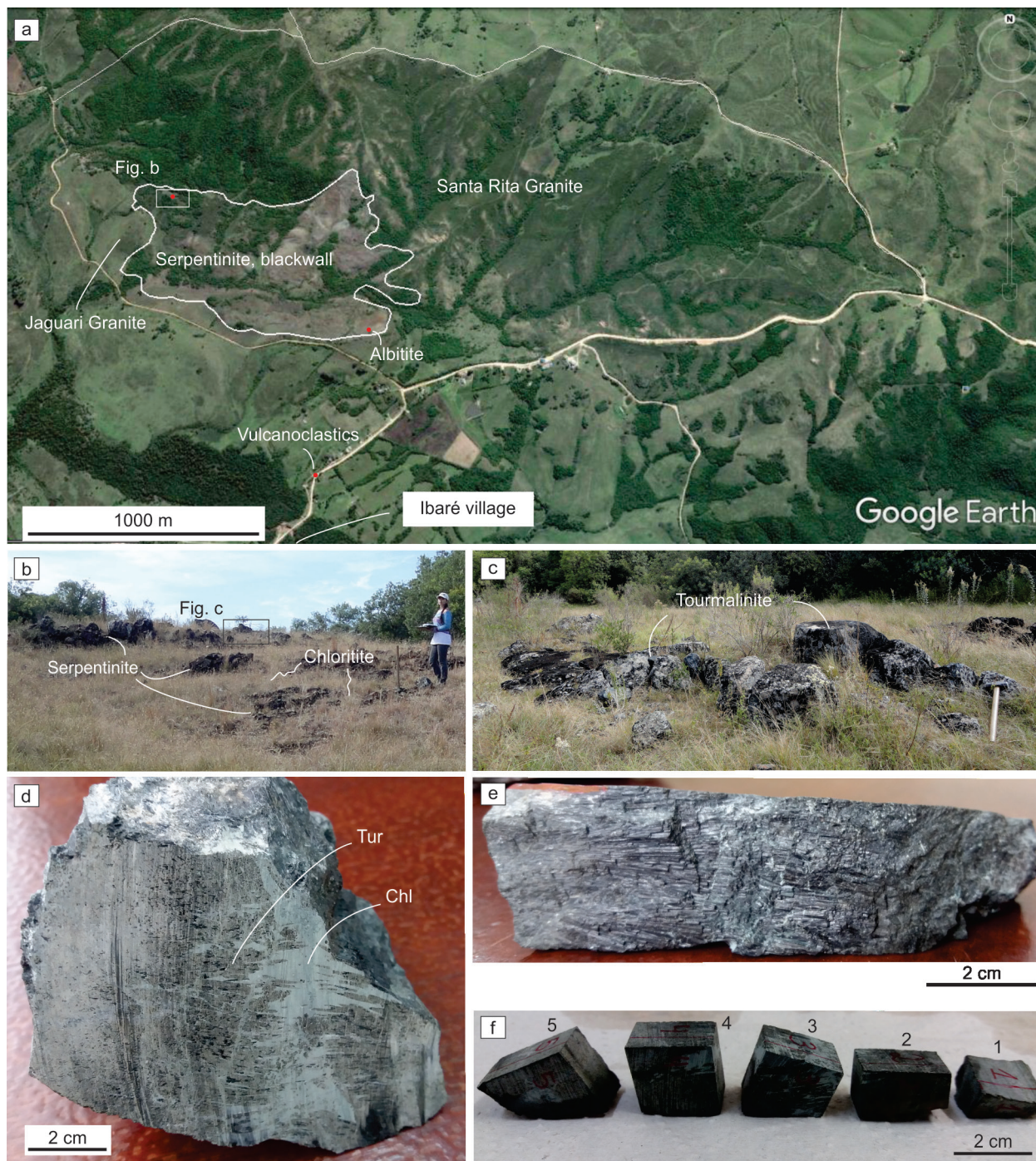


Figure 2. (a) Satellite image (Lansat 7) of study area; (b) Selected field of studied tourmalinite. Inset shows location of tourmalinite; (c) Studied tourmalinite outcrop; (d) Tourmalinite hand sample highlighting interfingering with chlorite; (e) Detail of tourmalinite, 10 cm long and 1.5 cm wide, cut from sample shown in Figure 2d; (f) Sectioned tourmalinite blocks for EPMA and LA-ICP-MS studies, shown as originally positioned in Figure 2e. Tur = tourmaline; Chl = chlorite.

the data were monitored during the analyses using dravite (#108796) and elbaite (#98144) (Leeman & Tonarini 2001) as external reference material (Supplementary Material - Table SII). The observed internal precision for individual analyses varied between 0.3 and 0.9‰.

Geological setting

The Brazilian Shield is composed of cratons and the Brasiliano Orogen, covering large extensions of eastern South America (e.g., Hartmann & Delgado 2001, Santos et al. 2019). The orogen is 4,000 x 1,500 km and comparable in many aspects to the accretionary to collisional Himalaya orogen. The orogen (900-550 Ma) has juvenile and crustally-reworked terranes. An intensively studied section is the juvenile São Gabriel belt, part of the Dom Feliciano Belt in the southern extension of the Brasiliano Orogen. The Ibaré ophiolite from the São Gabriel belt is part of the Dom Feliciano Belt (Figs. 1a, b). The formation of the Dom Feliciano Belt involved the closure of the Adamastor Ocean (Hartnady et al. 1985, Basei et al. 2018). Corresponding subduction events resulted in the development of two intra-oceanic arcs in the São Gabriel belt at the pre-collisional stage of the Brasiliano orogenic cycle (Machado et al. 1990, Leite et al. 1998, Remus et al. 1999, Gubert et al. 2016, Arena et al. 2017) with subsequent ophiolite emplacement (Arena et al. 2016, 2017). The Capané ophiolite occurs in the eastern portion of Dom Feliciano Belt (Fig. 1b) and has similar age to the São Gabriel belt (e.g., Arena et al. 2018). This ophiolite was emplaced into the Porongos fold and thrust belt (Pertille et al. 2015, 2017).

The main geological units of the São Gabriel belt formed in the Brasiliano Orogen (948 Ma to 660 Ma; Chemale et al. 1995, Babinski et al. 1996, Leite et al. 1998, Saalman et al. 2005a, b, Hartmann et al. 2011, Lena et al. 2014, Lopes et al. 2015, Arena et al. 2016). The studied tourmalinite

is part of the Ibaré ophiolite (Arena et al. 2017), associated with volcano-sedimentary rocks which are remnants of a Tonian intra-oceanic arc.

The Ibaré ophiolite and associated rocks (Figs. 1b, 2a) show evidence of regional greenschist facies metamorphism strongly overprinted by contact metamorphism caused by the intrusion (Naumann & Hartmann 1984, Naumann 1985) of the Santa Rita Granite (584.7 ± 1.9 Ma - Arena et al. 2017). Zircon U-Pb-Hf isotopic and geochemical characteristics of the Ibaré tourmalinite (Arena et al. 2017) indicate the beginning of metasomatism at 880 Ma, culminating with the ophiolite emplacement at 722 Ma into intra-oceanic arc in subduction-zone setting along the margins of the Rio de la Plata craton.

Sample description

Within the Ibaré ophiolite, massive tourmalinite (>90 vol.% tourmaline) is associated with chloritite, serpentinite, magnesian schist, rodingite, and albitite (Naumann 1985, Arena et al. 2016, 2017). Santa Rita Granite intruded the ophiolite in the northern portion and a tongue of the Jaguari Granite intruded in the southern portion. The tourmalinite (2 x 5 m large) occurs immersed in chloritite and serpentinite (Figs. 2b, c). Black color of tourmalinite is distinctive and contrasts with serpentinite and the surrounding chloritite blackwall. The tourmalinite is composed of tourmaline, chlorite, some ilmenite and zircon.

RESULTS

Representative electron microprobe analyses of tourmaline are listed in Supplementary Material - Table SIII. All analyzed points ($n = 60$) in tourmaline showed chemical homogeneity.

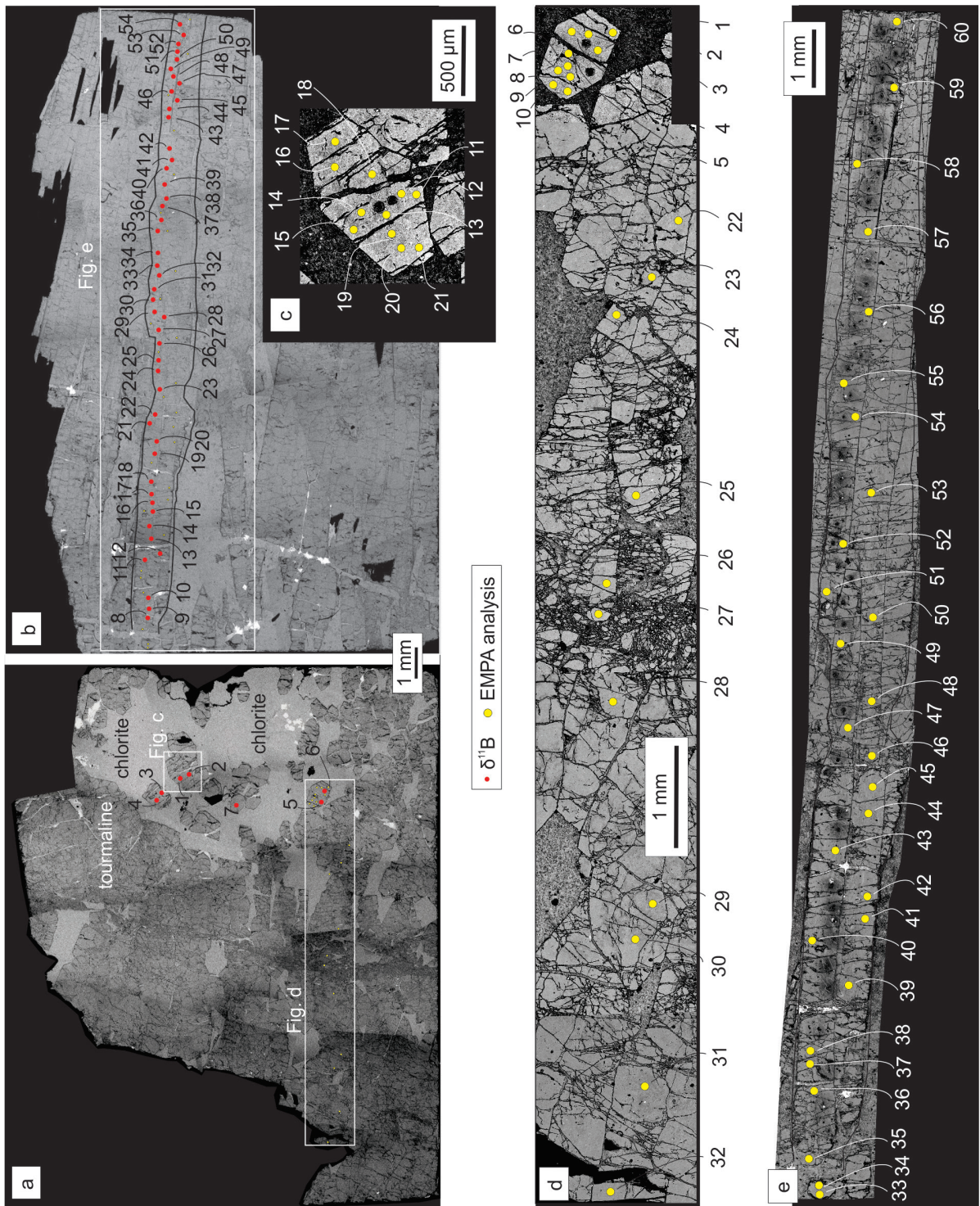


Figure 3. Back-scattered electron images of tourmalinite. (a) Section of block 3 (see Figure 2f) with location of $\delta^{11}\text{B}$ analyses; location of Figures 3c, d indicated; (b) Section of block 4 (Figure 2f) with location of $\delta^{11}\text{B}$ analyses; location of Figure 3e indicated; (c) Cross-section of dravite crystal indicating location of EPMA analyses. (d) Prism section of dravite crystals indicating location of EPMA analyses; one cross-section in extreme right; (e) Prism section of tourmaline crystals indicating location of EPMA analyses.

We made 21 analyses in two basal sections of individual tourmaline grains (Figs. 3c, d), 11 random tourmaline analyses (Fig. 3d) and 28 analyses along a tourmaline of approximately 20 mm length (Fig. 3e). They show a range in MgO from 7.16 to 8.64 wt.%, FeO from 6.25 to 7.76 wt.%, CaO from 0.22 to 0.49 wt.% and Na_2O from 2.54 to 2.80 wt.%.

The basic formula of tourmaline can be written as $\text{XY}_3\text{Z}_6(\text{T}_6\text{O}_{18})(\text{BO}_3)_3\text{V}_3\text{W}$, where X = Na, Ca, K, vacancy; Y = Fe^{2+} , Mg, Mn^{2+} , Li, Al, Cr^{3+} , V^{3+} , Fe^{3+} , Ti^{4+} ; Z = Mg, Al, Fe^{3+} , V^{3+} , Cr^{3+} ; T = Si, Al, (B); V = OH, O; W = OH, F, O (Hawthorne & Henry 1999). Chemical substitutions in tourmaline occur mainly in the X, Y and Z sites (Henry and Guidotti 1985). Some Al deficiency (<6 atoms per formula unit) in the Z site is due to Mg substitution and no Fe^{3+} . In addition, the X site occupancy is predominantly Na. The tourmaline is dravite in composition (Supplementary Material - Table SIII) and shows no chemical zoning (e.g., Fig. 4). Tourmalines are of alkali group (Na + K dominant at X site) and Mg-rich (Figs. 5a, b). The array is most consistent with operation of the MgFe^{2+}_{-1} substitution (Figs. 6a, b).

The studied IB14 tourmalines show homogenous isotopic compositions ranging from $\delta^{11}\text{B} = +3.5$ to $+5.2\text{‰}$ (Fig. 8b, Table I).

DISCUSSION

Dravite from Ibaré tourmalinite (IB14 sample) is Mg-rich and shows homogeneous chemistry and boron isotopic composition. Because tourmalinites may also form during regional and contact metamorphism, careful evaluation is necessary to determine their origin relative to hydrothermal, metamorphic and granitic process. Particular care is required for the identification of processes in the oceanic realm.

A previous study of metasomatic zircon from sample IB14 indicated positive $\epsilon\text{Hf} = +12.06$

to $+4.54$ over time, a signature interpreted as MORB fluid source (Arena et al. 2017). Most intense processes of zircon formation occurred at 722 Ma.

The Jaguari (569 ± 6 Ma; Gastal et al. 2015) and Santa Rita (584.7 ± 1.9 Ma; Arena et al. 2017) granites (Fig. 2) were considered possible sources in case tourmalinization occurred in the continent, after the emplacement of the ophiolite. Our results discard this hypothesis. Tourmaline in most granites and pegmatites in the continents has $\delta^{11}\text{B}$ values close to average continental crust ($\delta^{11}\text{B} = -10 \pm 3\text{‰}$; Marschall and Jiang 2011). Besides, tourmaline compositions in granitic rocks plot in fields 1 to 3 (Figs. 7a, b). In contrast, IB14 tourmalines plot in field 6 on Al-Fe-Mg(total) and Ca-Fe-Mg(total) diagrams (Henry & Guidotti 1985), unrelated to granitic rocks.

Chemistry of tourmalinite from seafloor volcano-exhalative activity (Beljavskis et al. 2005) shows that distal tourmalines plot into field 6 and proximal tourmalines overlap fields 2, 4 and 5 (Fig. 7a). In Figure 7b, distal tourmalines plot in field 7 reflecting high CaO content. Boron isotope compositions of tourmaline (Garda et al. 2009) in Ribeira belt tourmalinites previously studied by Beljavskis et al. (2005), showed $\delta^{11}\text{B} = -7.51$ to -14.58‰ . This evidences chemical and isotopic differences from the Ibaré tourmalinite (Figs 7a, b, 8b).

Tourmalines from Borborema pegmatites (Trumbull et al. 2013) overlap fields 5 and 6 on Al-Fe-Mg diagram (Fig. 7a); on Ca-Fe-Mg diagram (Fig. 7b), they overlap fields 1, 2 and 6 because of their preserved source chemical signature from surrounding rocks. The full range of $\delta^{11}\text{B}$ is -20.2 to $+1.6\text{‰}$ with main range -17 to -9‰ (Fig. 8b). Trumbull et al. (2013) suggest that the strong isotopic contrast between the main range and the heavy B resulted from mixing with enclosing marble and calc-silicate gneisses. It is significant

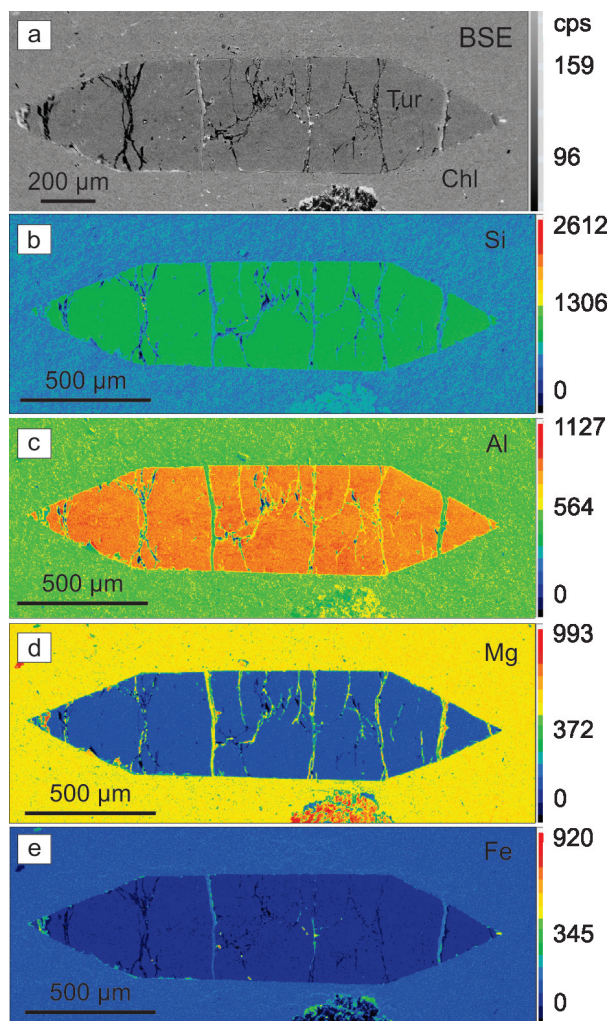


Figure 4. (a) Back-scattered electron image; (b-e) Characteristic X-ray map displaying the distribution of Si, Al, Mg, Fe in sample IB14. No compositional zoning observed. cps = count per second. Tur = tourmaline; Chl = chlorite.

that the origin of IB14 tourmaline was unrelated to granitic fluids. Ibaré tourmaline is Mg-rich but no associated sedimentary or exhalative rocks were identified. Tourmalines from many environments are strongly zoned and varied in trace elements and boron isotopes, but IB14 tourmaline is chemically homogeneous (Figs. 4, 7, 8). The uniformity in composition of IB14 tourmalines is highlighted by comparison with tourmalines from tourmalinites associated with augengneiss, leucogranite and garnet-micaschist

(Figs. 7a, b) (Menderes Massif, Turkey - Yücel-Öztürk et al. 2015).

In hydrothermal systems (Slack et al. 1993), Mg-rich tourmalines may form either by pre-metamorphic replacement from seawater-derived fluids under high fluid/rock conditions, or by sulfide-silicate reactions during metamorphism. Our results are more consistent with seawater-derived fluids. The IB14 dravite is interpreted as formed from entrained seawater (Slack & Trumbull 2011) (Fig. 7c) which caused serpentinization and subsequent tourmalinization.

The IB14 dravite has boron isotope composition ($\delta^{11}\text{B} = +3.5$ to $+5.2$ ‰) typical of blackwall metasomatism between altered oceanic crust and serpentinite. The tourmalinite formed below the seawater-sediment (or volcanic) interface with no exhalative component (closely associated or in contact with chemical sediments such as metachert and iron-formation) as described by Slack et al. (1993). This is in agreement with the values of modern bulk oceanic crust (Fig. 8a) by Farber et al. (2015), which range between $+3.7$ ‰ and $+7.9$ ‰ (Smith et al. 1995, Yamaoka et al. 2015). The B isotope composition of IB14 tourmalinite is more enriched in $\delta^{11}\text{B}$ than the slab materials from which they likely originated ($\delta^{11}\text{B}$ MORB = -3 ‰ to -14 ‰, average -7.1 ‰; Chaussidon & Jambon 1994, Marschall et al. 2017). This enrichment indicates that hydrothermal marine fluids altered bulk oceanic crust in the Ibaré tourmalinite. The boron concentration of fresh MORB has a $\delta^{11}\text{B}$ value of -7 ‰, but when circulating seawater interacts with ocean crust at ~ 100 °C, then the boron is taken up into secondary minerals. Compilations of ocean cores and ophiolite sections give average boron contents of $\delta^{11}\text{B} = +3$ ‰ for the upper oceanic crust (Smith et al. 1995) and the upper mantle may be altered to serpentinite by circulating

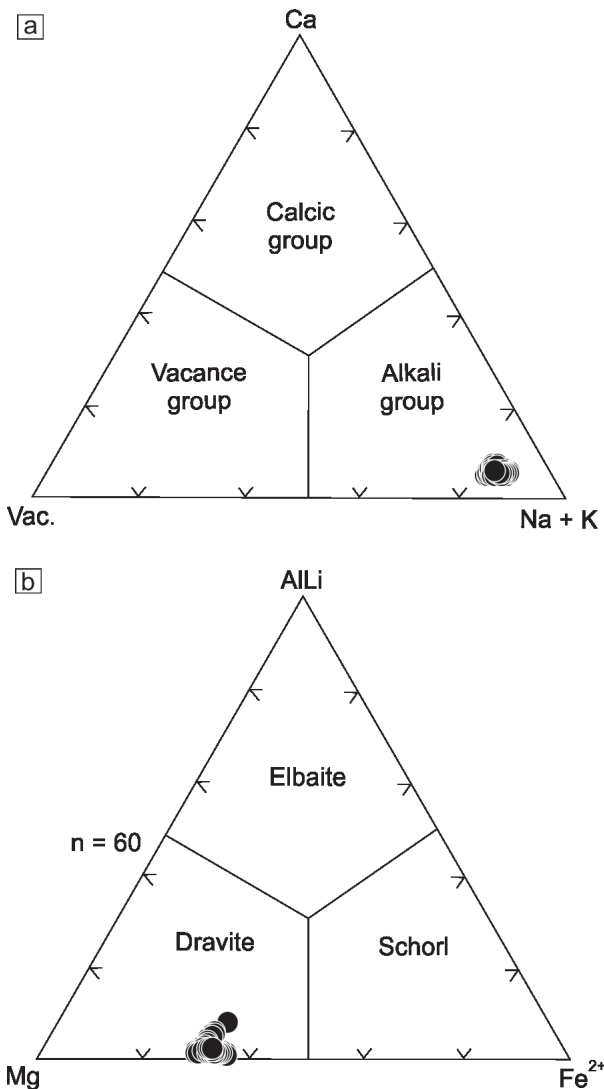


Figure 5. Ternary diagram using electron microprobe data. (a) Division according to the dominant occupancy of the X site to give the X-site vacant, alkali and calcic groups; (b) Classification of alkali group tourmaline with dominant occupancy of the Y site, highlighting dravite end member.

Table I. $\delta^{11}\text{B}$ results for tourmaline from tourmalinite, Ibaré ophiolite.

Spot	$d^{11}\text{B}$ (‰)	Spot	$d^{11}\text{B}$ (‰)
1	4.0 ± 0.18	28	4.1 ± 0.15
2	4.3 ± 0.18	29	4.0 ± 0.16
3	3.7 ± 0.19	30	4.0 ± 0.16
4	4.4 ± 0.18	31	3.9 ± 0.15
5	5.0 ± 0.19	32	3.7 ± 0.15
6	4.8 ± 0.19	33	4.0 ± 0.15
7	4.7 ± 0.20	34	3.6 ± 0.16
8	5.2 ± 0.14	35	3.6 ± 0.15
9	5.1 ± 0.14	36	3.6 ± 0.15
10	4.9 ± 0.14	37	3.5 ± 0.16
11	5.0 ± 0.13	38	3.6 ± 0.15
12	4.8 ± 0.14	39	3.7 ± 0.16
13	4.3 ± 0.17	40	3.7 ± 0.15
14	4.6 ± 0.14	41	4.1 ± 0.15
15	4.5 ± 0.15	42	4.1 ± 0.16
16	4.5 ± 0.15	43	4.0 ± 0.15
17	4.4 ± 0.15	44	4.5 ± 0.18
18	4.6 ± 0.14	45	4.4 ± 0.15
19	4.0 ± 0.15	46	4.5 ± 0.19
20	4.3 ± 0.14	47	4.6 ± 0.19
21	4.6 ± 0.13	48	4.7 ± 0.19
22	4.4 ± 0.14	49	4.5 ± 0.19
23	4.2 ± 0.14	50	4.5 ± 0.18
24	4.4 ± 0.13	51	4.9 ± 0.18
25	4.2 ± 0.14	52	4.9 ± 0.18
26	4.0 ± 0.15	53	4.7 ± 0.18
27	4.3 ± 0.15	54	4.3 ± 0.19

seawater, particularly at slow-spreading mid-ocean ridges (Palmer 2017).

The boron isotopes composition of the oceanic crust is the result of crust interaction with seawater, through capture of boron during hydrothermal alteration (Spivack & Edmond 1987, Smith et al. 1995). The average $\delta^{11}\text{B}$ calculated for altered oceanic crust is +3.7‰

(Smith et al. 1995) while serpentinite shows $\delta^{11}\text{B}$ values ranging between +8 (Boschi et al. 2008) and +15.1‰ (Benton et al. 2001). An increase in heavy $\delta^{11}\text{B}$ values (+20‰; Harvey et al. 2014) occurs by interaction with hot hydrothermal fluids at low pH in deeper levels of the oceanic crust (Seyfried & Ding 1995). Tourmaline from

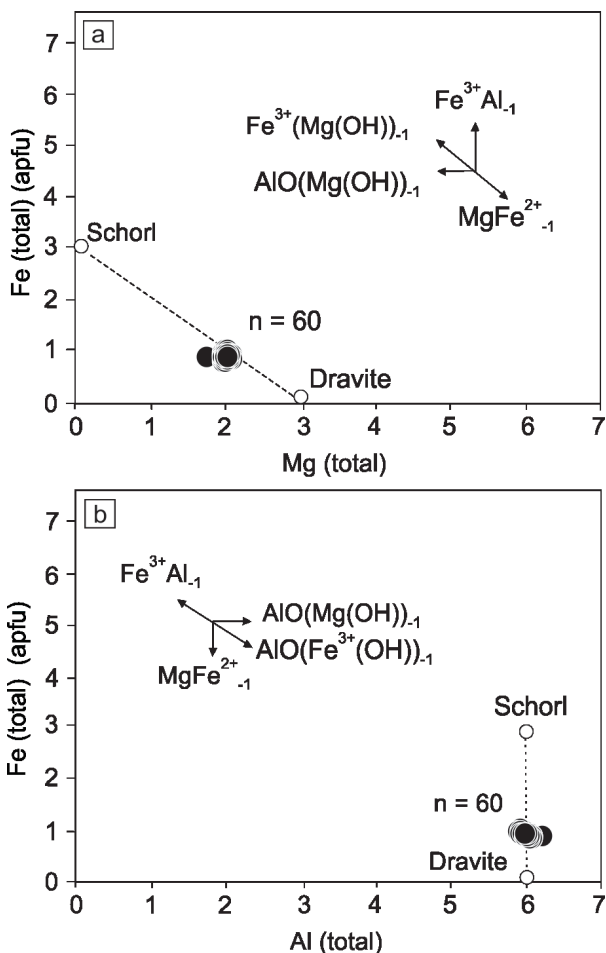


Figure 6. Diagrams of tourmalines from the Ibaré tourmalinite. (a) Mg versus Fe (total = Fe^{2+}). The dotted lines represent joins between selected end members. The array of data is along the schorl–dravite join (more Mg-rich) and is most consistent with operation of the MgFe^{2+}_{-1} substitution; (b) Al (total) versus Fe (total). The data classify the tourmaline as dravite end-member.

some geological settings may carry B enriched in ^{11}B (Table II).

The range in sediments is typically negative (except carbonates from +13.3‰ to +31.9‰, Hemming & Hönisch 2007). The older marine sediments analyzed by Ishikawa and Nakamura (1993) showed $\delta^{11}\text{B}$ values between -17‰ and -5.6‰, systematically lower than modern sediments.

An evaluation is made of the mobility of boron in subduction-zone environments to test

the hypotheses of origin of Ibaré tourmalinite. Boron isotopes can be used to unravel transfer processes from the subducting oceanic crust to the mantle wedge and to arc magmatism (Palmer 1991, Ishikawa & Tera 1999, Rosner et al. 2003, Savov et al. 2005). Studies by Ishikawa & Tera (1999) suggested a central role of altered oceanic crust and sediments as sources of fluids and boron in subduction zones. Additionally, Savov et al. (2005) and Tonarini et al. (2007) showed the potential role of subducted serpentinites as an important source of B-rich fluids to supra-subduction setting. Peacock & Hervig (1999) suggest that subduction-zone metamorphic dehydration reactions decrease the $\delta^{11}\text{B}$ value of subducted altered oceanic crust as well as subducted sediments through continuous dehydration reactions (Table II). Boron uptake in oceanic rocks occurs by direct incorporation of boron during crystallization of structurally favorable, B-rich hydrothermal-diagenetic minerals (phyllosilicates - Williams et al. 2001) or by adsorption from seawater by secondary minerals such as clays and during low-temperature interaction of fluids with crustal, mantle and sedimentary rocks (You et al. 1996). Chemical and boron isotopic characteristics of subduction-zone mobility of elements were not observed in Ibaré samples.

The isotopic and geochemical characteristics of IB14 dravite indicate parental fluid sourced from seawater. Lithospheric mantle was intensely metasomatized by large volumes of fluids during associated serpentinization (Fig. 8b). The characteristic depleted mantle composition of zircon contained in the tourmalinite and chloritite (Arena et al. 2017) supports the derivation of studied tourmaline from altered oceanic crust.

We envisage a geological history of the Ibaré ophiolite starting with oceanic crust formation in the Tonian during initial rifting of Rodinia.

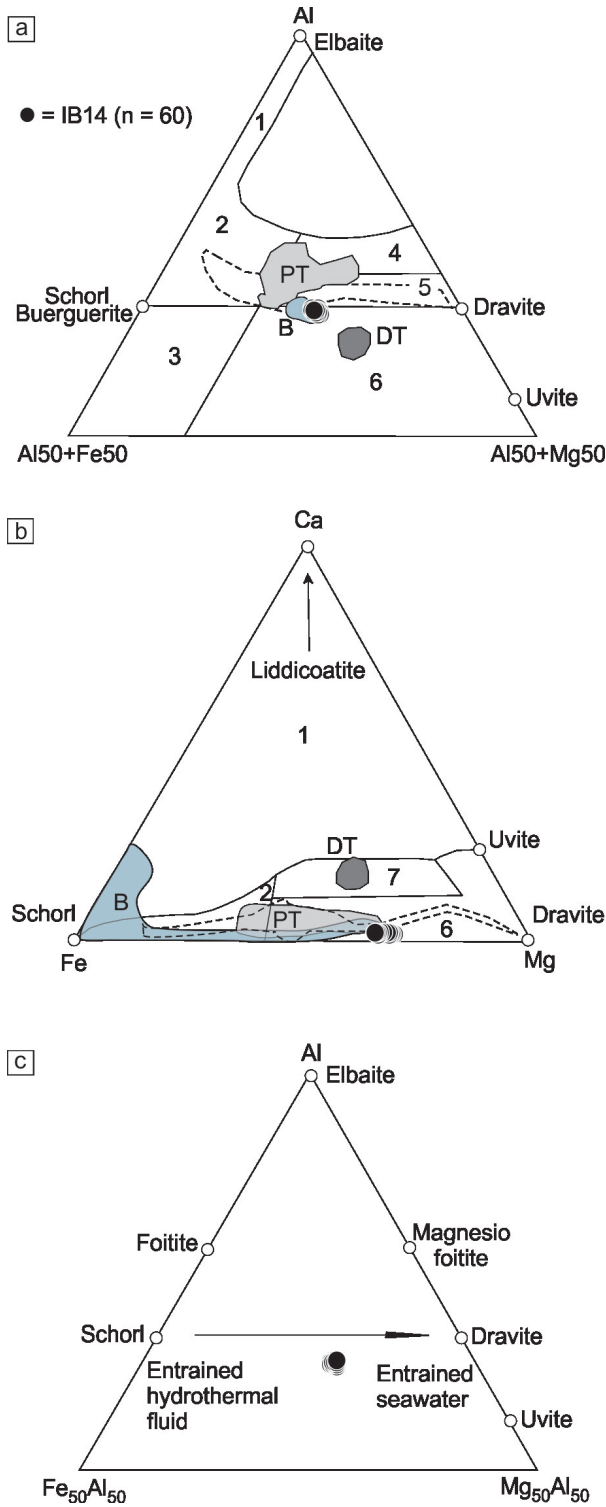


Figure 7. (a), (b) Plots of tourmalines on Al-Fe-Mg(total) and Ca-Fe-Mg(total) diagrams (after Yücel-Öztürk et al. 2015), 1 = Li-rich granitoid pegmatite and aplite, 2 = Li-poor granitoid and their associated pegmatite and aplite, 3 = hydrothermally altered granite, 4 = metapelite and metapsammite coexisting with an Al-saturated phase, 5 = metapelite and metapsammite not coexisting with an Al-saturated phase, low-Ca metaultramafic and Cr, V-rich metasediment, 6 = metacarbonate, metaultramafic, Fe³⁺-rich quartz-tourmaline rock, calc-silicate rock and Ca-poor metapelite, 7 = Ca-rich metapelite and calc-silicate rock; (c) Composition of tourmaline from the IB14 tourmalinite, indicating dominance of Mg-rich seawater over Fe-rich hydrothermal fluid. DT = distal tourmaline; PT = proximal tourmaline from Garda et al. (2009); B = Borborema tourmaline by Trumbull et al. (2013); dotted area = Yücel-Öztürk et al. (2015).

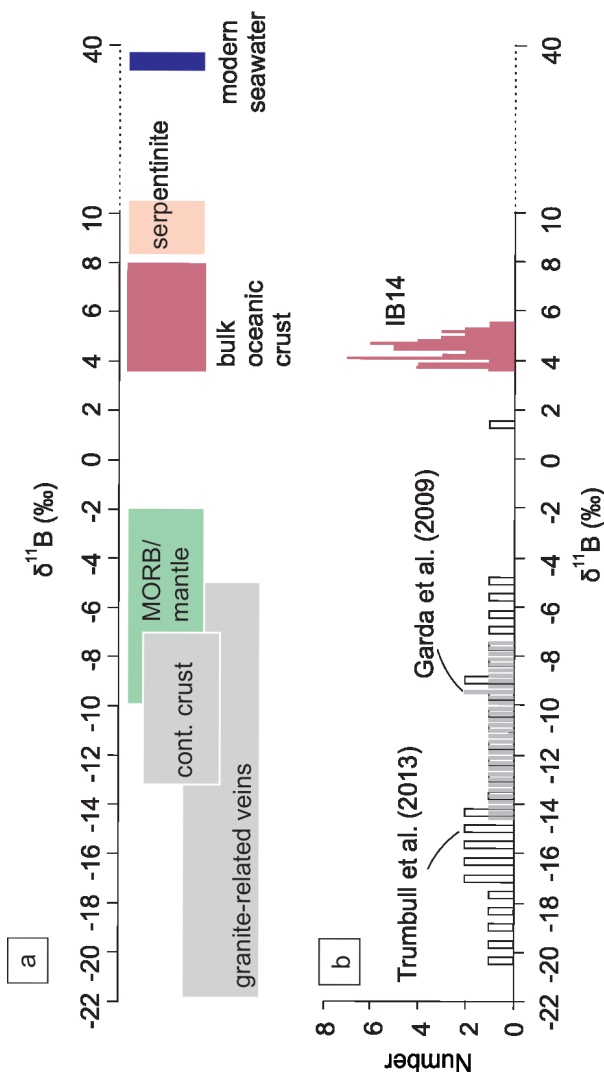


Figure 8. Histogram showing $\delta^{11}\text{B}$. (a) Different geological settings of boron sources (Farber et al. 2015); (b) Frequency histogram for IB14 tourmaline and data from literature.

Intense alteration of oceanic crust and mantle by interaction with heated oceanic water produced an association of serpentinite, chloritite blackwall and massive tourmalinite. This association was later accreted to an island-arc with little additional alteration of the tourmaline, which remained homogeneous in chemistry and boron isotopes. The characterization of the paleo-oceanic crust and mantle in the Ibaré ophiolite through the study of tourmalinite is most useful

Table II. B isotopes from selected geological settings.

Geological setting	$\delta^{11}\text{B}$ (‰)
Modern seawater	^a +40‰
Marine evaporite and carbonate	^a +18 to +32‰
Non-marine evaporite and carbonate	^a -30 to +7‰
Terrigenous marine sediments	^a -4 to +3‰
Altered oceanic crust	^a 0 to +13‰
Fresh oceanic crust	^a -3‰
Island arc volcanic rocks	^a -5 to +6‰
Andes arc volcanic rocks	^b -7 to +4‰
Continental reservoir	^c -20 to -7‰
Subduction zone	^d -11 to -3‰
This work	^e +3.5 to +5.2‰

^aPalmer & Slack, (1989), ^bRosner et al. (2003) ^cChaussidon & Albarède, (1992), ^dPeacock & Hervig, 1999, ^eThis work.

for the understanding of processes related to Rodinia rupturing and Gondwana assembly.

CONCLUSION

Dravite with no chemical zoning and with homogeneous isotopic composition ($\delta^{11}\text{B} = +3.5$ to $+5.2$ ‰) strengthens previous studies of mantle origin for intensely metasomatized Ibaré ophiolite. Tourmalines originated during formation of Neoproterozoic-Cambrian Brasiliano Orogen in oceanic altered crust prior to subduction and ophiolite obduction. Characterization of tourmalinite in Ibaré ophiolite is important to interpretations of geodynamic evolution of the southern Brasiliano Orogen.

Acknowledgments

This study is part of the PhD thesis by Karine da Rosa Arena at Programa de Pós-Graduação em Geociências, Universidade Federal do Rio Grande do Sul, Brazil. Karine held a scholarship during her PhD research from

Conselho Nacional de Desenvolvimento Científico e Tecnológico (CNPq). Financial support was provided by grant from Fundação de Amparo à Pesquisa do Estado do Rio Grande do Sul (FAPERGS) to Léo A. Hartmann. Reviewer João Orestes S. Santos is thanked for significant contributions that improved the manuscript.

REFERENCES

- ARENA KR, HARTMANN LA & LANA C. 2016. Evolution of Neoproterozoic ophiolites from the southern Brasiliano Orogen revealed by zircon U-Pb-Hf isotopes and geochemistry. *Precamb Res* 285: 299-314.
- ARENA KR, HARTMANN LA & LANA C. 2017. Tonian emplacement of ophiolites in the southern Brasiliano Orogen delimited by U-Pb-Hf isotopes of zircon from metasomatites. *Gondwana Res* 49: 296-332.
- ARENA KR, HARTMANN LA & LANA C. 2018. U-Pb-Hf isotopes and trace elements of metasomatic zircon delimit the evolution of neoproterozoic Capané ophiolite in the southern Brasiliano Orogen. *Int Geol Rev* 60: 911-928.
- BABINSKI M, CHEMALE JRF, HARTMANN LA, VAN SCHMUS WR & SILVA LC. 1996. Juvenile accretion at 750–700 Ma in Southern Brazil. *Geology* 24: 439-442.
- BASEI MAS, FRIMMEL HE, CAMPOS NETO MC, GANADE DE ARAUJO CE, CASTRO NA & PASSARELLI CR. 2018. The Tectonic History of the Southern Adamastor Ocean Based on a Correlation of the Kaoko and Dom Feliciano Belts. In: Siegesmund et al. (Eds), *Geology of Southwest Gondwana, Regional Geology Reviews*. Springer International Publishing AG, part of Springer Nature, 63-85.
- BELJAVSKIS P, GARDA GM, MANSUETO MS & SILVA D. 2005. Turmalinitos vulcanogênicos da Formação Morro da Pedra Preta do Grupo Serra do Itaberaba (SP): Petrografia, composição química da turmalina e implicações metalogenéticas. *Geologia USP-Série Científica* 5: 1-18.
- BENTON LD, RYAN JG & TERA F. 2001. Boron isotope systematics of slab fluids as inferred from a serpentine seamount, Mariana forearc. *Earth Planet Sci Lett* 187: 273-282.
- BOSCHI C, DINI A, FRÜH-GREEN GL & KELLEY DS. 2008. Isotopic and element exchange during serpentinization and metasomatism at the Atlantis Massif (MAR 30° N): insights from B and Sr isotope data. *Geochim Cosmochim Acta* 72: 1801-1823.
- CABRAL AR, TUPINAMBÁ M, ZEH A, LEHMANN B, WIEDENBECK M, BRAUNS M & KWITKO-RIBEIRO R. 2017. Platiniferous gold-tourmaline aggregates in the gold-palladium belt of Minas Gerais, Brazil: implications for regional boron metasomatism. *Mineral Petrol* 111: 807-819.
- CATANZARO EJ, CHAMPION CE, GARNER EL, MARINENKO G, SAPPENFIELD KM & SHIELDS WR. 1970. Standard reference materials: boric acid: isotopic and assay standard reference materials. U.S. National Bureau of Standards, Special Publication 70: 260-17.
- CHEMALE JRF, HARTMANN LA & DA SILVA LC. 1995. Stratigraphy and tectonism of the Brasiliano Cycle in southern Brazil. *Communs geol. Surv. Namibia* 10: 153-168.
- CHEMALE JRF, PHILIPP RP, DUSSIN AI, FORMOSO MLL, KAWASHITA K & BERTTOTTI AL. 2011. Lu-Hf and U-Pb age determination of Capivarita Anorthosite in the Dom Feliciano Belt, Brazil. *Precamb Res* 186: 117-126.
- CHAUSSIDON M & ALBARÈDE F. 1992. Secular boron isotope variations in the continental crust: an ion microprobe study. *Earth Planet Sci Lett* 108: 229-241.
- CHAUSSIDON M & JAMBON A. 1994. Boron content and isotopic composition of oceanic basalts: geochemical and cosmochemical implications. *Earth and Planetary Science Letters* 121: 277-291.
- DEVULDER V, GERDES A, VANHAECKE F & VANHAECKE P. 2015. Validation of the determination of the B isotopic composition in Roman glasses with laser ablation multi-collector inductively coupled plasma-mass spectrometry. *Spectrochimica Acta Part B* 105: 116-120.
- FARBER K, DZIGGEL A, TRUMBULL RB, MEYER FM & WIEDENBECK M. 2015. Tourmaline B-isotopes as tracers of fluid sources in silicified Palaeoarchean oceanic crust of the Mendon Formation, Barberton greenstone belt, South Africa. *Chem Geol* 417: 134-147.
- GARDA GM, TRUMBULL RB, BELJAVSKIS P & WIEDENBECK M. 2009. Boron isotope composition of tourmalinite and vein tourmalines associated with gold mineralization, Serra do Itaberaba Group, central Ribeira Belt, SE Brazil. *Chem Geol* 264: 207-220.
- GASTAL MC, FERREIRA FJF, CUNHA JU, ESMERIS C, KOESTER E, RAPOSO MIB & ROSSETTI MMM. 2015. Alojamento do granito Lavras e a mineralização aurífera durante evolução de centro vulcano-plutônico pós-colisional, oeste do Escudo Sul-riograndense: dados geofísicos e estruturais. *Braz J Geol* 45: 217-241.
- GUBERT ML, PHILIPP RP & BASEI MAS. 2016. The Bossoroca Complex, São Gabriel Terrane, Dom Feliciano Belt, southernmost Brazil: U-Pb geochronology and tectonic implications for the Neoproterozoic São Gabriel Arc. *J South Am Earth Sci* 70: 1-17.

- HARTMANN LA & DELGADO IM. 2001. Cratons and orogenic belts of the Brazilian Shield and their associated gold deposits. *Mineral Depos* 36: 207-217.
- HARTMANN LA, PHILIPP RP, SANTOS JOS & MCNAUGHTON NJ. 2011. Time frame of the 753–680 Ma juvenile accretion during the São Gabriel orogeny, southern Brazilian Shield. *Gond Res* 19: 84-99.
- HARTNADY CJH, JOUBERT P & STOWE C. 1985. Proterozoic crustal evolution in southwestern Africa. *Episodes* 8: 236-244.
- HARVEY J, SAVOV IP & AGOSTINI S. 2014. Si-metasomatism in serpentinized peridotite: the effects of talc-alteration on strontium and boron isotopes in abyssal serpentinites from Hole 1268a, ODP Leg 209. *Geochim Cosmochim Acta* 126: 30-48.
- HAWTHORNE FC & HENRY DJ. 1999. Classification of the minerals of the tourmaline group. *Eur J Mineral* 11: 201-215.
- HEMMING NG & HÖNISCH B. 2007. Boron isotopes in marine carbonate sediments and the pH of the ocean. *Develop Marine Geol* 1: 717-734.
- HENRY DJ & GUIDOTTI CV. 1985. Tourmaline as a petrogenetic indicator mineral: an example from the staurolite-grade metapelites of NW Maine. *Amer Mineral* 70: 1-15.
- HENRY DJ, NOVÁK N, HAWTHORNE FC, ERTL A, DUTROW BL, UHER P & PEZZOTTA F. 2011. Nomenclature of the tourmaline-super-group minerals. *Amer Mineral* 96: 895-913.
- ISHIKAWA T & NAKAMURA E. 1993. Boron isotope systematics of marine sediments. *Earth Planet Sci Lett* 117: 567-580.
- ISHIKAWA T & TERA F. 1999. Two isotopically distinct fluid components involved in the Mariana arc: evidences from Nb/B ratios and B, Sr, Nd, and Pb isotopes systematics. *Geology* 27: 83-86.
- LEEMAN WP & TONARINI S. 2001. Boron isotopic analysis of proposed borosilicate mineral reference samples. *Geostand Geoanalyst Res* 25: 399-403.
- LEITE JAD, HARTMANN LA, MCNAUGHTON NJ & CHEMALE JRF. 1998. SHRIMP U/Pb zircon geochronology of Neoproterozoic juvenile and crustal-reworked terranes in southernmost Brazil. *Int Geol Rev* 40: 688-705.
- LENA LOF, PIMENTEL MM, PHILIPP RP, ARMSTRONG R & SATO K. 2014. The evolution of the Neoproterozoic São Gabriel juvenile terrane, southern Brazil based on high spatial resolution U-Pb ages and $\delta^{18}\text{O}$ data from detrital zircons. *Precamb Res* 247: 126-138.
- LOPES CG, PIMENTEL MM, PHILIPP RP, GRUBER L, ARMSTRONG R & JUNGES S. 2015. Provenance of the Passo Feio Complex, Dom Feliciano Belt: implications for the age of supracrustal rocks of the São Gabriel Arc, southern Brazil. *J South Am Earth Sci* 58: 9-17.
- MACHADO N, KOPPE JC & HARTMANN LA. 1990. A late Proterozoic U-Pb age for the Bossoroca belt, Rio Grande do Sul, Brazil. *J South Am Earth Sci* 3: 87-90.
- MARSCHALL HR & JIANG SY. 2011. Tourmaline isotopes: no element left behind. *Elements* 7: 313-319.
- MARSCHALL HR, WANLESS VD, SHIMIZU N, PHILIP AE, STRANDMANN PV, ELLIOTT T & MONTELEONE BD. 2017. The boron and lithium isotopic composition of mid-ocean ridge basalts and the mantle. *Geochim Cosmochim Acta* 207: 102-138.
- MÍKOVÁ J, KOŠLER J & WIEDENBECK M. 2014. Matrix effects during laser ablation MC ICP-MS analysis of boron isotopes in tourmaline. *J Analyt Atomic Spectr* 29: 903-914.
- NAUMANN MP. 1985. O complexo Vulcano-sedimentar-ultramáfico e granitoides da região de Ibaré. Master thesis, Universidade Federal do Rio Grande do Sul. (Unpublished).
- NAUMANN MP & HARTMANN LA. 1984. Cornubianitos ultramáficos e metassomatitos associados da região do Arroio Corticeira, Proceedings of the Congresso Brasileiro de Geologia 33th, Rio de Janeiro, Brazil, p. 4279-4290.
- PALMER MR. 1991. Boron isotopes systematics of hydrothermal fluids and tourmalines: A synthesis. *Chem Geol* 94: 111-121.
- PALMER MR. 2017. Boron cycling in subduction zones. *Elements* 13: 237-242.
- PALMER M & SLACK J. 1989. Boron isotopic composition of tourmaline from massive sulfide deposits and tourmalinites. *Contrib Mineral Petrol* 103: 434-451.
- PEACOCK SM & HERVIG RL. 1999. Boron isotopic composition of subduction-zone metamorphic rocks. *Chem Geol* 160: 281-290.
- PERTILLE J, HARTMANN LA, PHILIPP RP, PETRY TS & LANA CC. 2015. Origin of the Ediacaran Porongos Group, Dom Feliciano Belt, southern Brazilian Shield, with emphasis on whole rock and detrital zircon geochemistry and U-Pb, Lu-Hf isotopes. *J South Am Earth Sci* 64: 69-93.
- PERTILLE J, HARTMANN LA, SANTOS JOS, MCNAUGHTON NJ & ARMSTRONG R. 2017. Reconstructing the Cryogenian-Ediacaran evolution of the Porongos fold and thrust belt, Southern Brasiliano Orogen, based on zircon U-Pb-Hf-O isotopes. *Int Geol Rev* 59: 1532-1560.

- PHILIPP RP, MASSONNE HJ & CAMPOS RS. 2013. Peraluminous leucogranites of the Cordilheira Suite: A record of Neoproterozoic collision and the generation of the Pelotas Batholith, Dom Feliciano Belt, Southern Brazil. *J South Am Earth Sci* 43: 8-24.
- PLIMER IR 1987. The association of tourmalinite with stratiform scheelite deposits. *Mineral Depos* 22: 282-291.
- QUEIROGA GN, PEDROSA-SOARES AC, NOCE CM, ALKMIM FF, PIMENTEL MM, DANTAS E, MARTINS M, CASTAÑEDA C, SUITA MTF & PRICHARD H. 2007. Age of the Ribeirão da Folha ophiolite, Araçuaí Orogen: the U-Pb zircon (LA-ICPMS) dating of a plagiogranite. *Geonomos* 15: 61-65.
- RAPELA CW, PANKHURST RJ, CASQUET C, FANNING CM, BALDO EG, GONZÁLEZ-CASADO JM, GALINDO C & DAHLQUIST J. 2007. The Río de la Plata craton and the assembly of SW Gondwana. *Earth Sci Rev* 8: 49-82.
- REMUS MVD, MCNAUGHTON NJ & HARTMANN LA. 1999. Gold in the Neoproterozoic juvenile Bossoroca Volcanic Arc of Southernmost Brazil: isotopic constraints on timing and sources. *J South Am Earth Sci* 12: 349-366.
- ROSNER M, ERZINGER J, FRANZ G & TRUMBULL RB. 2003. Slab-derived boron isotope signatures in arc volcanic rocks from the Central Andes and evidence for boron isotope fractionation during progressive slab dehydration. *Geochem Geophys Geosyst* 4: 1-25.
- SAALMANN K, HARTMANN LA, REMUS MVD, KOESTER E & CONCEIÇÃO RV. 2005a. Sm-Nd isotope geochemistry of metamorphic volcano-sedimentary successions in the São Gabriel Block, southernmost Brazil: evidence for the existence of juvenile Neoproterozoic oceanic crust to the east of the Río de la Plata craton. *Precambr Res* 136: 159-175.
- SAALMANN K, REMUS MVD & HARTMANN LA. 2005b. Geochemistry and crustal evolution of volcano-sedimentary successions and orthogneisses in the São Gabriel block, Southernmost Brazil-relics of Neoproterozoic magmatic arcs. *Gond Res* 8: 143-161.
- SANTOS JOS, CHERNICOFF CJ, ZAPPETIINI EO, MCNAUGHTON NJ & HARTMANN LA. 2019. Large geographic and temporal extensions of the Río de la Plata Craton, South America and its metacratonic eastern margin. *Int Geol Rev* 61: 56-85.
- SAVOV IP, RYAN JG, D'ANTONIO M, KELLEY K & MATTIE P. 2005. Geochemistry of serpentinitized peridotites from the Mariana Forearc Conical Seamount, ODP Leg 125: Implications for the elemental recycling at subduction zones. *Geochem Geophys Geosyst* 6: 1-24.
- SEYFRIED WE & DING K. 1995. Phase Equilibria in Subseafloor Hydrothermal Systems: A Review of the Role of Redox, Temperature, pH and Dissolved Cl on the Chemistry of Hot Spring Fluids at Mid-Ocean Ridge. *Physical, Chemical, Biological and Geological Interactions, AGU Geophysical Monograph* 91: 248-272.
- SLACK JF, PALMER MR, STEVENS BPJ & BARNES RG. 1993. Origin and significance of tourmaline-rich rocks in the Broken Hill District, Australia. *Econ Geol* 88: 505-541.
- SLACK JF & TRUMBULL RB. 2011. Tourmaline as a recorder of ore-forming processes. *Elements* 7: 321-326.
- SMITH HJ, SPIVACK AJ, STAUDIGEL H & HART SR. 1995. The boron isotopic composition of altered oceanic crust. *Chem Geol* 126: 119-135.
- SPIVACK AJ & EDMOND JM. 1987. Boron isotope exchange between seawater and the oceanic crust. *Geochim Cosmochim Acta* 51: 1033-1043.
- TINDLE AG, BREAKS FW & SELWAY JB. 2002. Tourmaline in petalite-subtype granitic pegmatites: Evidence of fractionation and contamination from the Pakeagama Lake and Separation Lake areas of northwestern Ontario, Canada. *Canad Mineral* 40: 753-788.
- TONARINI S, PENNISI M, ADORNI-BRACCESI A, DINI A, FERRARA G, GONFIANTINI R, WIEDENBECK M & GRÖNING M. 2003. Intercomparison of boron isotope and concentration measurements: Part I: Selection, preparation and homogeneity tests of the intercomparison materials. *Geostand Newsl* 27: 21-39.
- TONARINI S, AGOSTINI S, DOGLIONI C, INNOCENTI F & MANETTI P. 2007. Evidence for serpentinite fluid in convergent margin systems: The example of El Salvador (Central America) arc lavas. *Geochem Geophys Geosyst* 8: 1-18.
- TRUMBULL RB, KRIENITZ MS, GOTTESMANN B & WIEDENBECK M. 2008. Chemical and boron-isotope variations in tourmalines from an S-type granite and its source rocks: the Erongo granite and tourmalinites in the Damara Belt, Namibia. *Contrib Mineral Petrol* 155: 1-18.
- TRUMBULL RB, BEURLLEN H, WIEDENBECK M & SOARES DR. 2013. The diversity of B-isotope variations in tourmaline from rare-element pegmatites in the Borborema Province of Brazil. *Chem Geol* 352: 47-62.
- VAN HINSBERG VJ, HENRY DJ & DUTROW BL. 2011. Tourmaline as a petrologic forensic mineral: a unique recorder of its geologic past. *Elements* 7: 323-332.
- WILLIAMS LB, HERVIG RL, HOLLOWAY JR & HUTCHEON I. 2001. Boron isotope geochemistry during diagenesis. Part I. Experimental determination of fractionation during

illitization of smectite. *Geochim Cosmochim Acta* 65: 1769-1782.

YAMAOKA K, ISHIKAWA T, MATSUBAYA O, ISHIYAMA D, NAGAISHI K, HIROYASU Y, CHIBA H & KAWAHATA H. 2012. Boron and oxygen isotope systematics for a complete section of oceanic crustal rocks in the Oman ophiolite. *Geochim Cosmochim Acta* 84: 543-559.

YAMAOKA K, MATSUKURA S, ISHIKAWA T & KAWAHATA H. 2015. Boron isotope systematics of a fossil hydrothermal system from the Troodos ophiolite, Cyprus: water-rock interaction of oceanic crust and subseafloor ore deposits. *Chem Geol* 396: 61-73.

YOU CF, SPIVACK AJ, GIESKES JM, MARTIN JB & DAVISSON ML. 1996. Boron contents and isotopic compositions in pore water: a new approach to determine temperature-induced artifacts-geochemical implications. *Marin Geol* 129: 351-361.

YÜCEL-ÖZTÜRK Y, HELVACI C, PALMER MR, ERSOY EY & FRESLON N. 2015. Origin and significance of tourmalinites and tourmaline-bearing rocks of Menderes Massif, western Anatolia, Turkey. *Lithos* 218-219: 22-36.

SUPPLEMENTARY MATERIAL

Table SI - Reference materials used for calibration of Electron Microprobe analyses.

Table SII - Boron isotopic analyses of secondary reference materials.

Table SIII - Electron Microprobe analyses of tourmaline from tourmalinite, Ibaré ophiolite.

How to cite

ARENA KR, HARTMANN LA, LANA CC, QUEIROGA GN & CASTRO MP. 2020. Geochemistry and $\delta^{11}\text{B}$ evolution of tourmaline from tourmalinite as a record of oceanic crust in the Tonian Ibaré ophiolite, southern Brasiliano Orogen. *An Acad Bras Cienc* 92: e20180193. DOI 10.1590/0001-3765202020180193.

Manuscript received on March 3, 2018; accepted for publication on October 31, 2019

KARINE DA ROSA ARENA¹

<https://orcid.org/0000-0002-5724-7333>

LÉO AFRANEO HARTMANN¹

<https://orcid.org/0000-0001-7863-5071>

CRISTIANO DE CARVALHO LANA²

<https://orcid.org/0000-0001-6302-9706>

GLÁUCIA NASCIMENTO QUEIROGA²

<https://orcid.org/0000-0002-1730-0638>

MARCO PAULO DE CASTRO²

<https://orcid.org/0000-0001-8209-5995>

¹Instituto de Geociências, Universidade Federal do Rio Grande do Sul, Avenida Bento Gonçalves, 9500, 91501-970 Porto Alegre, RS, Brazil

²Departamento de Geologia, Escola de Minas, Universidade Federal de Ouro Preto, Morro do Cruzeiro, 35400-000 Ouro Preto, MG, Brazil

Correspondence to: **Karine da Rosa Arena**

E-mail: karinearena@gmail.com

Author contributions

Karine da Rosa Arena did field work, prepared the samples, organized and interpreted the data, and wrote the text of the article. Léo Afraneo Hartmann participated in field work, samples study, supervision of data handling and revision of English of text. Cristiano Lana prepared samples, did $\delta^{11}\text{B}$ analyses on the LA-ICP-MS and reduced data. Gláucia N. Queiroga supervised EPMA analyses, and data reduction and interpretation. Marco P. Castro operated the EPMA for the analyses of minerals and participated in interpretation of data.

